Optimization of Electrooptic Sampling by Volume-Integral Method

W. Thomann, *Student Member, IEEE,* M. Rottenkolber, and P. Russer, *Senior Member, IEEE*

***Abstract*—A rigorous treatment of the influence of an inhomogeneous electric field on the differential polarization of an optical field, and the corresponding change in transmission of a retarder setup is presented. The method yields sensitivity coefficients employed directly in a volume-integral. In case of an external electrooptic probe tip a layered structure with a space-harmonic potential and a Gaussian sampling beam is investigated and results on sensitivity and spatial resolution are presented. The probing of inhomogeneous longitudinal and transverse fields with the same setup is demonstrated for a microstrip transmission line.**

I. Introduction

ELECTROOPTIC probing meets with growing interest for noncontact and noninvasive measurements of integrated microwave circuits. The exact knowledge of the influence of a microwave field in a planar circuit on the Gaussian optical probe beam is essential for accurate measurement. We describe a method for calculation of the sensitivity and the spatial resolution. Especially, in cases of electrooptic sampling utilizing a diode laser, sensitivity is of utmost importance. The issue of invasiveness is addressed by Nagatsuma *et al.* [1] and Frankel *et al.* [2]. The method presented is applicable to the case of direct probing in electrooptic active substrates and the use of an external electrooptic probe tip. The determination of the change in polarization, and the resulting intensity variations of the reflected sampling beam after passing a polarizer, are based on the rigorous application of the volume-integral method. The introduced method takes into account the Gaussian nature of the probing beam.

II. Sensitivity Coefficients

To calculate the change in transmission of an optical beam in an electrooptic sampling setup including polarizers, we introduce a method which yields 1) sensitivity coefficients representing a linear relationship between electrical fields and polarization of optical waves for arbitrary crystal orientation, and 2) their direct application to determine the change in transmission of the optical beam. We first calculate the differential change of polarization for an arbitrarily directed homogeneous field and for static isotrope uniaxial crystals. Consecutively, we employ the introduced sensitivity coefficients in a volume-integral method for the application of inhomogeneous fields. Fig. 1 depicts the crystal coordinate system $\boldsymbol{x}$, the eigenmode-system $\tilde{\boldsymbol{x}}$, with $\tilde{x}$ (ordinary eigenmode) and $\tilde{y}$ (extraordinary eigenmode), and the beam axis $\boldsymbol{e}_{\text{opt}}$ (parallel to $\tilde{z}$), using polar coordinates (θ, ψ). We choose $\boldsymbol{e}_{\tilde{x}} = \boldsymbol{e}_z \times \boldsymbol{e}_{\tilde{z}}$ and use a coordinate transformation $\boldsymbol{x} = \boldsymbol{A}\tilde{\boldsymbol{x}}(\boldsymbol{A}^T = \boldsymbol{A}^{-1})$ for further calculation. The impermeability tensor $\boldsymbol{b}$ of a uniaxial crystal and its electrooptic part $\boldsymbol{b}^{\text{EO}}$ (n_o—ordinary index of refraction, n_e—extraordinary index of refraction) with respect to $\boldsymbol{x}$ is given as:

$$\boldsymbol{b} = \begin{pmatrix} n_o^{-2} & 0 & 0 \\ 0 & n_o^{-2} & 0 \\ 0 & 0 & n_e^{-2} \end{pmatrix}; \qquad \boldsymbol{b}^{\text{EO}} = \begin{pmatrix} \delta_1 & \delta_6 & \delta_5 \\ \delta_6 & \delta_2 & \delta_4 \\ \delta_5 & \delta_4 & \delta_3 \end{pmatrix} \tag{1}$$

with $\delta_m = \Sigma_{k=1}^{3}\, r_{mk} E_k^m$ (r_{mk}—pockels coefficients, E_k^m—electric field components of microwave field). The transformed impermeability tensor using δ_{ij} (Kronecker-Delta) is

$$\beta = \boldsymbol{A}^T\left(\frac{\delta_{ij}}{n_t^2} + b_{ij}^{\text{EO}}\right)\boldsymbol{A} = \beta^{\text{stat}} + \beta^{\text{EO}}. \tag{2}$$

From Maxwell's equations, we obtain a wave equation for the dielectric displacement $\boldsymbol{D}$: $\nabla \times (\nabla \times \boldsymbol{bD}) - k_0^2 \boldsymbol{D} = 0$, and with respect to the direction of propagation $\boldsymbol{e}_{\text{opt}}$ we obtain a linear differential equation of first order:

$$\beta_t \frac{\partial^2 \boldsymbol{D}}{\partial \tilde{z}^2} = -k_0^2 \boldsymbol{D} \quad \text{and} \quad \frac{\partial \boldsymbol{D}}{\partial \tilde{z}} = \pm jk_0 \boldsymbol{N}\boldsymbol{D} \tag{3}$$

where $\boldsymbol{N}$ is the index of refraction matrix. We define $\boldsymbol{N}$ in such a manner that we obtain $\boldsymbol{N}^2\beta_t = \boldsymbol{I}$ (β_t—transverse components of β, $\boldsymbol{I}$—unity matrix):

$$\boldsymbol{N} = \begin{pmatrix} n_1 - \Delta n_1 & -\Delta n_3 \\ -\Delta n_3 & n_2 - \Delta n_2 \end{pmatrix}. \tag{4}$$

By comparison of $\boldsymbol{N}$ with β (2) and neglection of higher order products ($\Delta n_1 \Delta n_2$ etc.), we can determine the elements of the matrix $\boldsymbol{N}$.

A general solution of the coupled differential equation (3) is: $\boldsymbol{D} = \exp(jk_0 \boldsymbol{N} z)\boldsymbol{D}_o$ ($\boldsymbol{D}_o$—dielectric displacement

Manuscript received March 26, 1993; revised June 16, 1993. This work was supported by the Deutsche Forschungsgemeinschaft (DFG), Germany.

W. Thomann and M. Rottenkolber are with the Technische Universität München, Institut für Hochfrequenztechnik, München, Germany.

P. Russer is with the Technische Universität München, Institut für Hochfrequenztechnik, München, Germany, and Ferdinand-Braun-Institut für Höchstfrequenztechnik, Berlin, Germany.

IEEE Log Number 9212970.

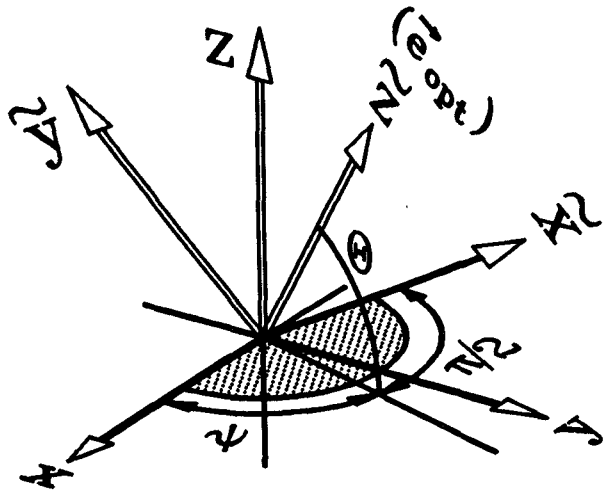

Fig. 1. Definition of the used coordinate systems.

vector before entering the crystal). Next, the change in polarization per unit length is described by the differential Jones matrix [3] of the EO-crystal. In case of linear birefringence without loss, we only need to consider the following two terms of the differential Jones matrix:

$$\Delta N = g_0 \begin{pmatrix} j & 0 \\ 0 & -j \end{pmatrix} + g_{45} \begin{pmatrix} 0 & j \\ j & 0 \end{pmatrix} \tag{5}$$

with g_0 (linear birefringence parallel to the eigenmode axis) and g_{45} (linear birefringence parallel to the angle bisector of the eigenmode axes). The rotated matrix $\Delta N(\varphi)$ is given by:

$$\Delta N(\varphi) = \begin{pmatrix} jg_0 & jg_{45} \\ jg_{45} & -jg_0 \end{pmatrix} \tag{6}$$

with $g_0 = g \cos(2\varphi)$, $g_{45} = g \sin(2\varphi)$, and $g = \sqrt{g_0^2 + g_{45}^2}$ which are combined in the differential retardation vector $\boldsymbol{g} = (g_0, g_{45})^T$, given by Thomas [4]. Assuming a differential retarder with a static and electrooptic plate $\boldsymbol{g} = \boldsymbol{g}_{\text{stat}} + \boldsymbol{g}_{\text{EO}}$ we can employ $\boldsymbol{g}$ to determine the change in transmission and we obtain with $\Gamma_B = \Gamma_0 + \Gamma_{C,\text{stat}}$ (Γ_B—total phase retardation (bias), 0—static, C—crystal, k_0—free space wave vector):

$$\Delta I = \sin \Gamma_B k_0 l \begin{pmatrix} \cos 2 \left(\varphi_0 - \frac{\pi}{4}\right) \\ \sin 2 \left(\varphi_0 - \frac{\pi}{4}\right) \end{pmatrix} \boldsymbol{g} \tag{7}$$

$$\Delta I_{C\text{stat}} = \tfrac{1}{2} \sin \Gamma_B k_0 l \begin{pmatrix} \sin 2\varphi_0 \\ -\cos 2\varphi_0 \end{pmatrix}^T \begin{pmatrix} n_1 - n_2 \\ 0 \end{pmatrix} \tag{8}$$

$$\Delta I_C^{\text{EO}} = \tfrac{1}{2} \sin \Gamma_B k_0 l \begin{pmatrix} \sin 2\varphi_0 \\ -\cos 2\varphi_0 \end{pmatrix}^T \begin{pmatrix} \Delta n_2 - \Delta n_1 \\ -2\Delta n_3 \end{pmatrix} \tag{9}$$

$$\Delta I_C^{\text{EO}} = \sin \Gamma_B k_0 l (\kappa_x E_x^m + \kappa_y E_y^m + \kappa_z E_z^m). \tag{10}$$

Equation (10) introduces the sensitivity coefficients [5] describing the linear dependence (κ_i, $i = x, y, z$) of the change in transmission caused by the electric field components E_x^m, E_y^m, E_z^m. As an example, we calculate the sensitivity coefficients K_{x_s}, K_{y_s}, K_{z_s} for perpendicular incidence in reflection mode and with respect to the substrate coordinate system $\boldsymbol{x}_s$:

$$\Delta I_C^{\text{EO}} = 2k_0 l \begin{pmatrix} \kappa_x \\ \kappa_y \\ \kappa_z \end{pmatrix}^T \boldsymbol{A}\boldsymbol{E}_{x_s} = k_0 l \begin{pmatrix} K_{x_s} \\ K_{y_s} \\ K_{z_s} \end{pmatrix} \boldsymbol{E}_{x_s}. \tag{11}$$

III. Sensitivity Coefficients of 3m-Systems and 43m-Systems

Fig. 2 depicts the sensitivity coefficients K_{x_s}, K_{y_s}, K_{z_s} for the 3m-crystals $LiTaO_3$ and $LiNbO_3$, and for perpendicular incidence in the reflection mode with respect to $\boldsymbol{x}_s$ and the angle θ (retarder angle φ_0 as parameter).

The diagrams emphasize the following statements: 1) due to the same electrooptic tensor structure we obtain maximum longitudinal sensitivity ($K_{z_s,\max}$) for both materials at an angle θ of 35° and a retarder angle φ_0 of 45° (which corresponds to the result of Aoshima [6] and Nagatsuma [7]), 2) $LiNbO_3$ exhibits a higher sensitivity compared to $LiTaO_3$, and 3) longitudinal and transverse probing can be realized with the same electrooptic setup, simply by changing the retarder angle φ_0 [5]. However, for a given crystal cut $\theta = 35°$ ($\varphi = 45°$) we can only realize a quasi-longitudinal probe since the coefficient K_{y_s} is not zero, i.e., a transverse component $K_{y_s} E_{y_s}^m$ is present. This effect can be compensated by performing two measurements with a different retarder angle at the same probing location. For a quasi-static microwave field (negligible field components in y_s-direction of propagation) we can omit the second measurement, and 4) for the angles $\theta = 35°$ and $\varphi = 45°$, we obtain maximum sensitivity for an angle ψ of $-90°$.

Table I shows some of the important transverse and quasi-longitudinal probing cases of $LiTaO_3$ and $LiNbO_3$ (3m-system) as well as for GaAs ($\bar{4}3$m-system) and $Bi_{12}SiO_{20}$ (42-system). In case of thick $Bi_{12}SiO_{20}$ crystals, an offset caused by optical activity can be taken into account by appropriate adjustment of the analyzer. An optimized external probe tip (3m-systems) for longitudinal field components $\boldsymbol{E}_{z_s}^m$ is realized with a crystal cut θ of 35°. Fig. 3 depicts the corresponding crystal angles. In a similar manner, we obtain the sensitivity coefficients of $\bar{4}3$m-systems given in Table I. As in the case of 3m-systems, we can employ the same probing setup for transverse and longitudinal probing simply by changing the retarder angle φ_0, if we use a crystal cut with $\theta = 45°$. For the longitudinal case, we need an angle θ of 90° which corresponds for $\psi = -90°$ to the direct longitudinal probing in (001)-GaAs.

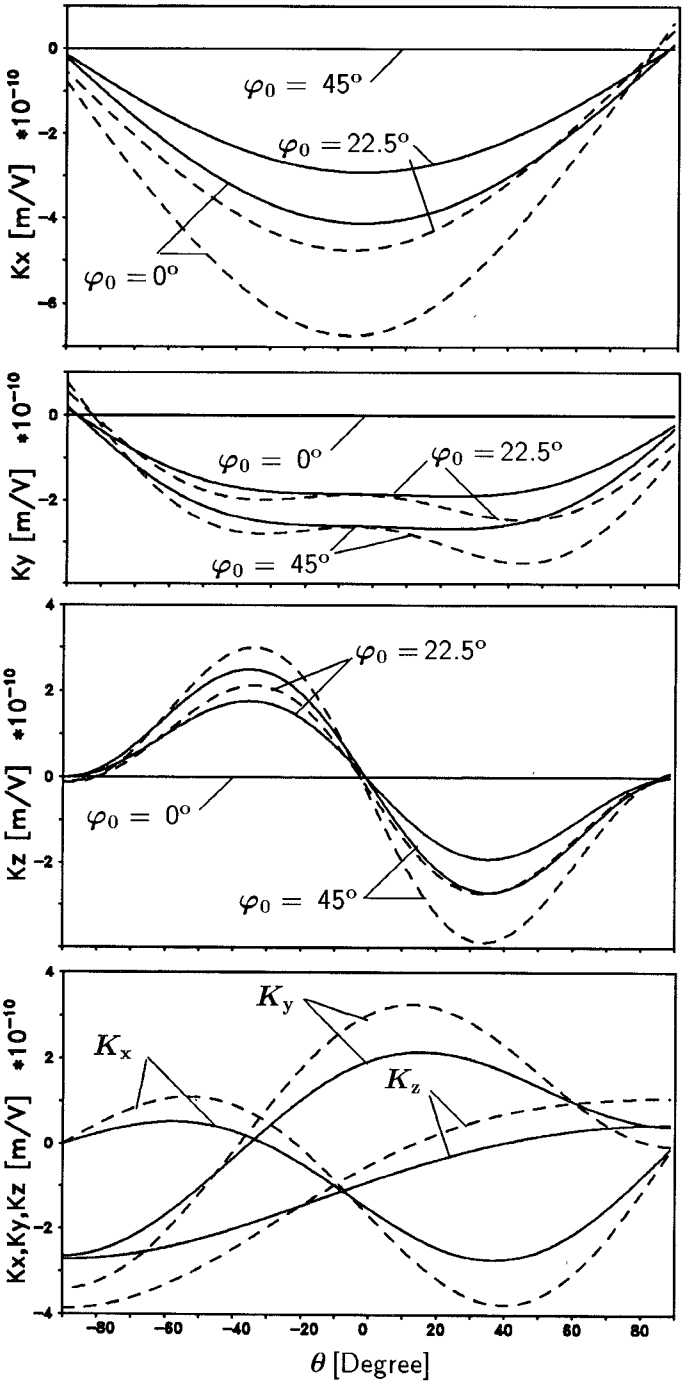

Fig. 2. K_{x_s}, K_{y_s}, K_{z_s} of $LiTaO_3$ (solid) and $LiNbO_3$ (dashed) with $\psi = -90°$ (upper three diagrams) and $\theta = 35°$ and $\varphi_0 = 45°$ (lower diagram).

Applying the previously described method, we obtain the total change in transmission ΔI as:

$$\Delta I = \frac{\sin \Gamma_B}{2} k_0 \int_0^l \boldsymbol{K}^T \boldsymbol{E}_{x_s} \, d\tilde{z} \tag{12}$$

which is valid for a plane-wave sampling beam of infinitesimal diameter. Due to the latter assumption, transverse inhomogeneities of $\boldsymbol{E}_{x_s}$ are not included.

TABLE I
SENSITIVITY COEFFICIENTS OF TRANSVERSE AND QUASI-LONGITUDINAL PROBING IN $LiTaO_3$, $LiNbO_3$, GaAs AND $Bi_{12}SiO_{20}$

Material/ Symmetry	φ_0	θ	ψ	K_{x_s}	K_{y_s} $\cdot 10^{-10}$ m/V	K_{z_s}
$LiTaO_3$ 3m	0°	35°	−90°	−3.26	0	0
	45°	35°	−90°	0	−2.64	−2.71
	45°	35°	−35°	0.152	0	−1.89
$LiNbO_3$ 3m	0°	35°	−90°	−4.91	0	0
	45°	35°	−90°	0	−3.41	−3.87
	45°	35°	−38°	0.85	0	−2.38
GaAs $\bar{4}3m$	0°	90°	−90°	0	0	−1.13
	0°	45°	−90°	0	−1.13	−1.13
	45°	45°	−90°	−1.13	0	0
$Bi_{12}SiO_{20}$ 42	0°	90°	−90°	0	0	−1.64
	0°	45°	−90°	0	−1.64	−1.64
	45°	45°	−90°	−1.64	0	0

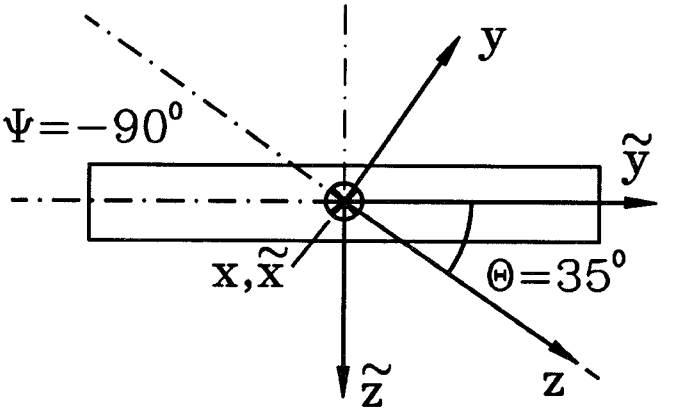

Fig. 3. Crystal cut $\theta = 35°$ (see 3m-system) and orientation of coordinate systems for realization of a sensitivity optimized probe tip for longitudinal field component $E_{z_s}^m$.

IV. VOLUME-INTEGRAL METHOD

The general description of the interaction of any optical field and inhomogeneous microwave field can be derived by applying a perturbation ansatz to the Lorentz-reciprocity theorem as shown by Monteath [8]. The results [4], [9] of this approach can be expressed as a change of optical transmission given by:

$$\Delta S_{BA} = -\frac{jk_0}{2n} \int_{\text{Vol}} \boldsymbol{e}^{(-)} \Delta\boldsymbol{\varepsilon} \boldsymbol{e}^{(+)'} \, dV. \tag{13}$$

For derivation of this expression, the interaction of an optical field and microwave field is described by a two-aperture-system (general twoport) shown in Fig. 4 with aperture A and B. The field amplitude transmission coefficient ΔS_{BA}, describes the change in transmission of the optical field due to a small perturbation of the dielectric tensor $\Delta\boldsymbol{\varepsilon}$ with $\Delta\boldsymbol{\varepsilon} = \boldsymbol{\varepsilon}' - \boldsymbol{\varepsilon}$.

The probing geometry in reflection mode (reflection at the rear surface of external probe crystal or electrooptic substrate) is reduced to a transmission mode with a crystal

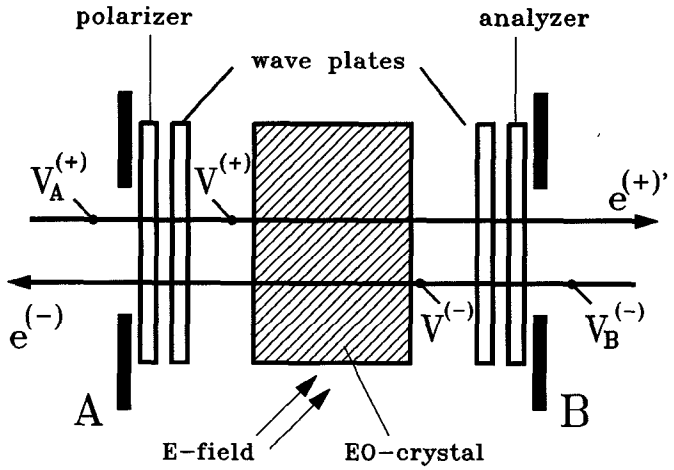

Fig. 4. Two-aperture system in transmitting mode.

of twice the length ($2l$). The polarizing elements are assumed to be infinitesimally thin and close to the EO-crystal. The optical field traveling from B to A and normalized to the incident power at aperture B is denoted $e^{(-)}$. Conversely, the optical field traveling from aperture A to aperture B and normalized to the incident power at aperture A, in presence of a perturbation caused by a microwave field, is denoted $e^{(+)'}$. Since the perturbation is assumed to be very small, we can replace $e^{(+)'}$ by $e^{(+)}$ as shown by Freeman [9]. Thus, the normalized change in transmission in presence of a microwave field is expressed as:

$$\Delta I = I' - I = S'_{BA}S'^{*}_{BA} - S_{BA}S^{*}_{BA}$$
$$= 2Re\{S^{*}_{BA}\Delta S_{BA}\}. \tag{14}$$

S_{BA} represents the transmission without electrooptic induced perturbation and can be replaced by the bias-point value $S_{BA} = \sin(\Gamma_B/2)$ without introducing restrictions. Thus we obtain:

$$\Delta I = 2\sin\frac{\Gamma_B}{2} Re\left\{-\frac{jk_0}{2n}\int_{\text{Vol.}} e^{(-)T}\Delta\varepsilon\, e^{(+)}\, dV\right\}. \tag{15}$$

In the following, we assume 1) a circularly symmetric Gaussian beam solely described by its transverse components and 2) polarization of the Gaussian beam described by Jones vectors and weighed by the Gaussian field distribution.

These assumptions allow the use of the Jones-matrix formalism for the determination of the polarization of the (+) and (−) wave before entering the crystal in the static state. The change $\Delta\varepsilon$ with respect to the static eigenmode system, is derived from the index of refraction matrix for the static case (N) and under influence of an electric field (N'). With $\Delta\varepsilon = \varepsilon' - \varepsilon = N'^2 - N^2$, we obtain the change of the dielectric tensor as:

$$\Delta\varepsilon = \begin{pmatrix} -n_1^4\beta_{11}^{\text{EO}} & -\bar{n}^4\beta_{12}^{\text{EO}} \\ -\bar{n}^4\beta_{12}^{\text{EO}} & -n_2^4\beta_{22}^{\text{EO}} \end{pmatrix} \tag{16}$$

with neglection of higher order modes in β_{ij}^{EO} and the approximation $\bar{n}^4 \doteq n_1^3n_2^2/(n_1+n_2) \doteq n_1^2n_2^3/(n_1+n_2)$.

Under the previously stated assumptions the fields $e^{(+)}$ and $e^{(-)}$ can be expressed with Jones vectors as follows: $e^{(+)} = V^{(+)}|e^{(+)}|$ and $e^{(-)} = V^{(-)}|e^{(-)}|$. The magnitudes of incident wave $|e^{(+)}|$ and reflected wave $|e^{(-)}|$ are equal. Thus, for the calculation of $e^{(+)}$ and $e^{(-)}$ we only have to consider the Jones vectors of the (+) and (−) wave at the aperture A and B, denoted $V^{(+)}$, $V^{(-)}$, and $V_A^{(+)}$, $V_B^{(+)}$, respectively. With respect to the static eigenmode system we obtain:

$$V_A^{(+)} = \frac{1}{\sqrt{2}}\begin{pmatrix}1\\1\end{pmatrix} \tag{17}$$

$$V_B^{(+)} = W_{\text{an.}}\, W(\tfrac{1}{2}\Gamma_0, 0)\, W_C(\Gamma_C, 0)\, W(\tfrac{1}{2}\Gamma_0, 0)\, V_A^{(+)} \tag{18}$$

with the Jones matrices of the analyzer $W_{\text{an.}}$ and the EO-crystal W_C and the wave plates W. The Jones matrix of the polarizer can be neglected due to appropriate normalization and with $\rho^2 = \exp(j(\Gamma_C/2))\exp(j(\Gamma_0/2)) = \exp(j(\Gamma_B/2))$, we obtain:

$$V_B^{(+)} = \frac{\rho^2 - \rho^{*2}}{2\sqrt{2}}\begin{pmatrix}1\\-1\end{pmatrix} = \frac{jS_{BA}}{\sqrt{2}}\begin{pmatrix}1\\-1\end{pmatrix} \tag{19}$$

$$V_B^{(-)} = \frac{V_B^{(+)}e^{-j\delta}}{|V_B^{(+)}|} = \frac{1}{\sqrt{2}}\begin{pmatrix}1\\-1\end{pmatrix}. \tag{20}$$

With an arbitrarily chosen phase factor $\delta = -\pi/2$ for $V_B^{(+)}$, we obtain a real vector for $V_B^{(-)}$. With $\rho_0 = \exp(j\Gamma_0/4)$, we obtain:

$$V^{(+)} = W\left(\frac{1}{2}\Gamma_0, 0\right) V_A^{(+)} = \frac{1}{\sqrt{2}}\begin{pmatrix}\rho_0\\ \rho_0^*\end{pmatrix} \tag{21}$$

$$V^{(-)} = W\left(\frac{1}{2}\Gamma_0, 0\right) V_B^{(-)} = \frac{j}{\sqrt{2}}\begin{pmatrix}\rho_0\\ \rho_0^*\end{pmatrix}. \tag{22}$$

An arbitrary retarder angle φ_0 is taken into consideration by rotation of the dielectric tensor: $\Delta\varepsilon' = D(\varphi_0')\,\Delta\varepsilon D(-\varphi_0')$ and with $\varphi_0' = \varphi_0 - \pi/4$ we obtain:

$$e^{(-)T}\Delta\varepsilon' e^{(+)} = \frac{j}{2}|e^{(+)}|^2\left(\cos\frac{\Gamma_0}{2}(\Delta\epsilon'_{22} - \Delta\epsilon'_{11}) - j\sin\frac{\Gamma_0}{2}(\Delta\epsilon'_{22} + \Delta\epsilon'_{11})\right). \tag{23}$$

As shown by (15), we only consider the real part of (24) and with $\Delta I_{\text{norm}} = \sin(\Gamma_B/2)\cdot\cos(\Gamma_0/2)$, we obtain ΔI for the transmitting mode to:

$$\Delta I = \Delta I_{\text{norm}}\int_{\text{Vol.}}\begin{pmatrix}\sin 2\varphi_0\\ \cos 2\varphi_0\end{pmatrix}^T \cdot\begin{pmatrix}\Delta\epsilon_{22} - \Delta\epsilon_{11}\\ 2\Delta\epsilon_{12}\end{pmatrix}|e^{(+)}|^2\, dV \tag{24}$$

Comparison of (24) with (10) and (11) gives:

$$\begin{pmatrix} \sin 2\varphi_0 \\ -\cos 2\varphi_0 \end{pmatrix}^T \begin{pmatrix} n_1^4 \beta_{11}^{EO} - n_2^4 \beta_{22}^{EO} \\ 2\bar{n}^4 \beta_{12}^{EO} \end{pmatrix} = \bar{n} \begin{pmatrix} \kappa_x \\ \kappa_y \\ \kappa_z \end{pmatrix}^T \boldsymbol{E}^m = \frac{1}{2} \bar{n} \boldsymbol{K}^T \boldsymbol{E}_{x_s}^m \quad (25)$$

$$\overline{\Delta I} =: \frac{\Delta I}{\Delta I_{\text{norm}}} = \frac{k_0}{2\bar{n}} \int_{\text{Vol.}} \frac{1}{2} \boldsymbol{K}^T \boldsymbol{E}_{x_s}^m |e^{(+)}|^2 \, dV. \quad (26)$$

To determine the change in transmission we need to take into account the power-density distribution of the Gaussian sampling beam. However, we neglect the different beam waists in direction of the eigenmode axes.

In the following, we consider the perpendicular probing case and express the transverse electric field [10] of the beam:

$$e^{(+)} = \sqrt{\frac{2k_0}{\bar{n}b}} \frac{jb}{z' + jb} \cdot \exp\left(-jk_0\bar{n} \frac{x^2 + y^2}{2q(z)}\right) \cdot \exp\left(-jk_0\bar{n}(z - z_0)\right) \quad (27)$$

with the confocal parameter $b = w_0 \pi \bar{n}/\lambda_0 = w_0^2 k_0/2\bar{n}$ and $z' = z - z_0$ and $q(z) = z' + jb$. The position of the beam waist is denoted z_0 and the beam radius as a function of distance is given by $w(\xi) = w_0\sqrt{1 + \xi^2}$. With the confocal length $L = w_0^2 k_0 \bar{n}$ and $\xi = 2(z - z_0)/L$ we obtain:

$$g_1 = |e^{(+)}|^2 = \frac{2}{\pi w^2(\xi)} \exp\left(-2 \frac{x^2 + y^2}{w^2(\xi)}\right) \quad (28)$$

with $\xi_1 = 2(z_s - z_0)/L$ and $\xi_2 = 2(-z_s - z_0)/L$, before and after reflection, respectively. This results in the following expression [5] for the electrooptic-induced change in intensity:

$$\overline{\Delta I} = \frac{k_0}{2\bar{n}} \int_0^l \int_{-\infty}^{\infty} \int_{-\infty}^{\infty} \frac{1}{2} \boldsymbol{K}^T \boldsymbol{E}_{x_s}^m \cdot \{g_1(\xi_1) + g_1(\xi_2)\} \, dx_s \, dy_s \, dz_s. \quad (29)$$

It can be shown, that in case of slightly tilted beam (see Fig. 6), the sensitivity coefficients remain almost the same since the perturbation terms compensate each other. The approximate change in transmission is calculated for incident and reflected beam portions individually.

The sensitivity vector $\boldsymbol{K}$ with respect to a dimensionless vector $\boldsymbol{e}_{x_s}^m (|\boldsymbol{e}_{x_s}^m| = 1)$ of the electric field, yields the scalar product: $\boldsymbol{K}^T \boldsymbol{E}_{x_s} = \boldsymbol{K}^T \boldsymbol{e}_{x_s}^m |\boldsymbol{E}_{x_s}^m|$. In case of a tilted beam the product $|\boldsymbol{E}_{x_s}^m| g_1$ can be generalized to a scalar product of the vectors $|\boldsymbol{E}_{x_s}^m| g_1 = \boldsymbol{E}_{x_s} \boldsymbol{e}_{\text{opt}} g_1$ and we obtain the total

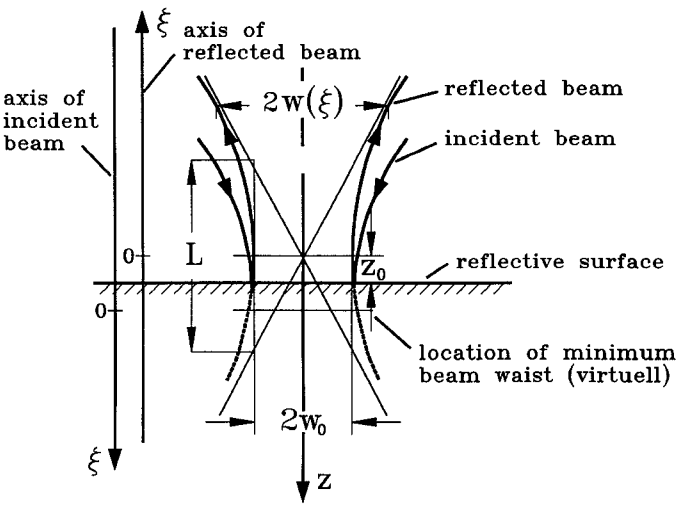

Fig. 5. Propagation of Gaussian beam within EO-crystal.

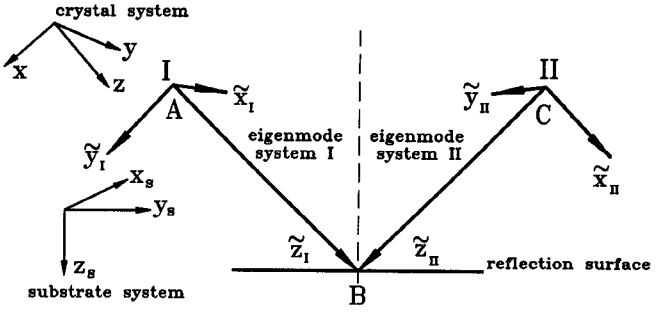

Fig. 6. General coordinate system of reflection mode probing.

intensity change in transmission:

$$\overline{\Delta I} = \frac{k_0}{2\bar{n}} \int_{A \to B} \int_{-\infty}^{\infty} \int_{-\infty}^{\infty} \frac{1}{2} \boldsymbol{K}^T \boldsymbol{e}_{x_s}^m \boldsymbol{E}_{x_s}^m \boldsymbol{e}_{\text{opt}}^I g_1^I \, dV_I + \frac{k_0}{2\bar{n}} \int_{C \to B} \int_{-\infty}^{\infty} \int_{-\infty}^{\infty} \frac{1}{2} \boldsymbol{K}^T \boldsymbol{e}_{x_s}^m \boldsymbol{E}_{x_s}^m \boldsymbol{e}_{\text{opt}}^{II} g_1^{II} \, dV_{II}. \quad (30)$$

In case of longitudinal probing ($K_x = K_y = 0$, $K_z \neq 0$), this equation can be simplified since $\boldsymbol{K}^T \boldsymbol{e}_{x_s}^m$ is independent of the integration variables. Furthermore, if the field can be expressed as the gradient of a scalar potential ($\boldsymbol{E}_{x_s} = \text{grad } V$) and the optical wave is a solenoid field [$\text{div}(\boldsymbol{e}_{\text{opt}} g_1) = 0$] we can apply the Gaussian theorem and the volume integral reduces to a surface integral:

$$\overline{\Delta I} = K_z \frac{k_0}{2\bar{n}} \int_{-\infty}^{\infty} \int_{-\infty}^{\infty} [(V_A g_{1A} \boldsymbol{e}_{\text{opt}}^I + V_C g_{1C} \boldsymbol{e}_{\text{opt}}^{II}) \boldsymbol{e}_z - 2V_B g_{1B} \boldsymbol{e}_{\text{opt}}^I \boldsymbol{e}_z] \, dx_s \, dy_s \quad (31)$$

i.e., ΔI only depends on the potentials V_A, V_C, and V_B at the upper and lower surface of the probing crystal, respectively, and weighed with the power distribution of the optical wave.

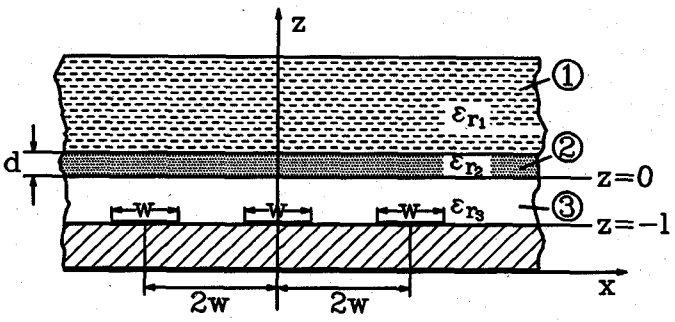

Fig. 7. Transverse periodic transmission lines with external electrooptic layer for determination of spatial resolution and sensitivity.

V. Evaluation of Space-Harmonic Potential

As an example, we apply the volume-integral method to external sampling in case of a static space harmonic potential (phase constant = 0). The fields of planar microwave transmission lines can be expressed as a gradient of a scalar potential for sufficiently low frequencies provided neglecting longitudinal field components: $E^m = \text{grad}\ \phi$. The structure and the coordinate system is shown in Fig. 7.

The electrooptic layer, as well as the lateral periodic transmission line structure (w), are assumed to be open. The EO-layer with a relative dielectric constant ϵ_{r2} is embedded between the top carrier layer (ϵ_{r1}) and an air gap (ϵ_{r3}), respectively. With the assumption of an exact cosine shape of the field components in x-direction the Helmholtz equation of the Hertzian vector reduces to the Laplace equation for the scalar potential. For calculation, we apply the following potential to the three layers: $\phi(x, z) = \phi_i \cos \alpha_0 x \cdot \cdots\ i = 1, 2, 3$ with $\phi_1 = Ae^{-\alpha_0(z+d)}$, $\phi_2 = Be^{-\alpha_0 z} + Ce^{\alpha_0 z}$, $\phi_3 = Ge^{-\alpha_0 z} - He^{\alpha_0 z}$, and $\alpha_0 = \pi/(2w)$. For a forced potential $\phi(x, z = -h) = V_0 \cos \alpha_0 x$ at $z = -h$, we can determine the field components E_{x2} and E_{z2} in the EO-active layer 2 [11]. Due to the assumption $E_y^m \doteq 0$, the integration in (29) can be performed with respect to y_s. As an example, we consider the purely longitudinal case which is possible for GaAs, and for (3m)-crystals like $LiTaO_3$ and $LiNbO_3$ ($\theta = 35°$): $K_x = K_y = 0$, and $K_z \neq 0$. We obtain the intensity variation ΔI at the probing position X to:

$$\overline{\Delta I}(X) = \frac{k_0}{2\bar{n}} \int_0^d \int_{-\infty}^{\infty} K_z E_z^m(x, z) \{ g_2(x - X, \xi_1) + g_2(x - X, \xi_2) \}\, dx\, dz \tag{32}$$

with

$$g_2(x, \xi_i) = \sqrt{\frac{2}{\pi}} \cdot \frac{\exp\left(-2\dfrac{x^2}{w^2(\xi_i)}\right)}{w(\xi_i)}. \tag{33}$$

Applying the Fourier transformation we obtain the spectral domain representation and we define a normalized transmission characteristic $H(\alpha) = \overline{\Delta I}(\alpha)/\tilde{\phi}(\alpha, z = -h)$ with respect to $\phi(x, z = -h)$ with a field-dependent term $E_z = f(C(\alpha))$ and $k = f(\epsilon_{r1}, \epsilon_{r2})$ [11]:

$$H(\alpha) = K_z \alpha C(\alpha) \int_0^d (ke^{-\alpha z} \cdot e^{2\alpha h} - e^{\alpha z}) \cdot (e^{-\alpha^2 w^2(\xi_1)/8} + e^{-\alpha^2 w^2(\xi_2)/8})\, dz \tag{34}$$

VI. External Electrooptic Probe

As an example, we choose GaAs with $n = 3.41$, $\lambda = 1.3\ \mu$m, and $\epsilon_{r1} = 1$, $\epsilon_{r2} = 13$, $\epsilon_{r3} = 1$. The results of $H(\alpha)/K_z(\alpha = \alpha_0$, local phase constant) are shown in Fig. 8 and Fig. 9. The transmission function $H(\alpha)$ exhibits a bandpass characteristic. The maximum H_{max} is between the space-frequency h^{-1} and d^{-1}. Thus, a reduction of sensitivity is caused by h and d. In practice, h must be chosen smaller than d.

The transmission function depends on geometrical and optical parameters [11] briefly described:

1) The sensitivity $|H(\alpha)|$, as well as the spatial resolution, are significantly dependant on the probe distance h. The maximum of $|H(\alpha)|$ at $h = 1\ \mu$m, compared to $h = 0.1\ \mu$m, reduces by a factor of 10. The sensitivity is reduced by a factor of 2 ($w_0 = 2\ \mu$m, $h = 10\ \mu$m, $z_0 = 0$, $d = 30\ \mu$m) for spatial frequency of $\alpha = 1.12 \cdot 10^5\ \text{m}^{-1}$ which corresponds to a line spacing of 14 μm.

2) An increase in electrooptic probe thickness d from 30–100 μm results in an increase of sensitivity of only 1.6 and only at lower spatial frequencies.

3) The maximum spatial resolution [3dB decrease of $H(\alpha)$] is for ideal conditions ($w_0 = 2\ \mu$m, $z_0 = 0$, $h = 1\ \mu$m, $d = 30\ \mu$m) $1.5 \cdot 10^5\ \text{m}^{-1}$ which corresponds to a line width w of 10.5 μm. For identical parameters, but a probe distance of $h = 0.1\ \mu$m, we obtain a minimum line width of $w = 4.9\ \mu$m.

4) The dielectric constant of layer 1 has no influence on the sensitivity at higher spatial frequencies due to the significant decay of the field components in the EO-crystal.

5) The sensitivity of the probe is determined only by the optical parameters (w_0, z_0) if the absolute value of h is small. An increase of minimum Gaussian radius from $w_0 = 2\ \mu$m to $w_0 = 5\ \mu$m, at higher spatial frequencies $\alpha = 9 \cdot 10^5\ \text{m}^{-1}$ results in a significant reduction of sensitivity by a factor of 10. The position z_0 of the beam waist within the EO-crystal only influences the spatial resolution at higher spatial frequencies.

VII. Probing of Arbitrary Inhomogeneous Transverse and Longitudinal Fields

The method presented can be applied to arbitrary inhomogeneous fields. As an example, we chose a 300 μm wide microstrip transmission line on a 400 μm thick GaAs substrate at a frequency of 1 GHz. The optimized external electrooptic probe (see Table I), of 100 μm thick $LiTaO_3$, is placed at a distance of 10 μm. The electric field components were calculated using spectral domain analysis (SDA) with a transversely unlimited structure.

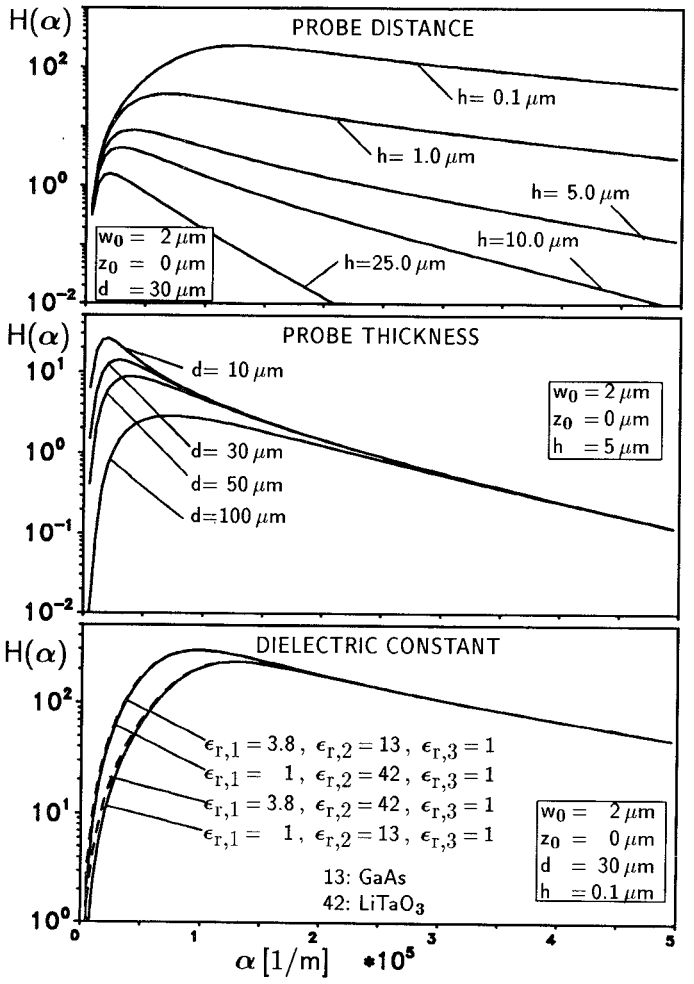

Fig. 8. Transmission characteristic $H(\alpha)$ with probe distance h, probe thickness d, and dielectric constants as parameter.

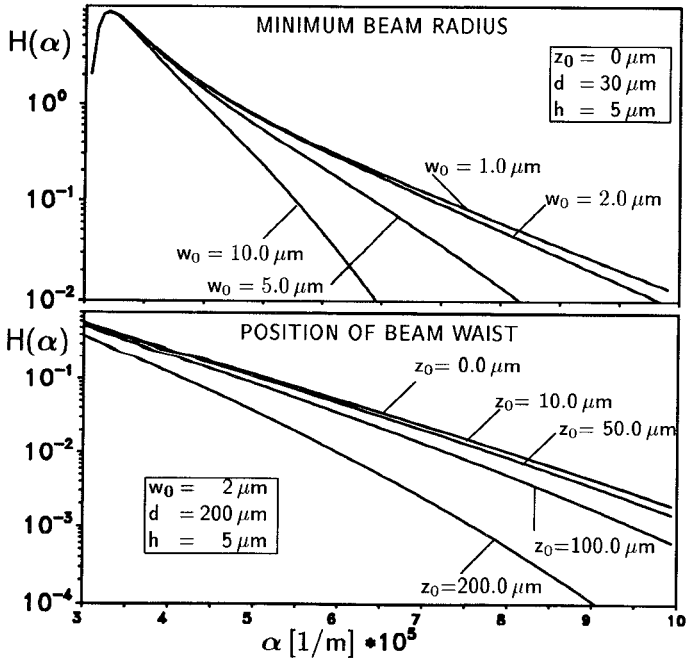

Fig. 9. Transmission characteristic $H(\alpha)$ with minimum beam radius w_0 and position of beam waist z_0 as parameter.

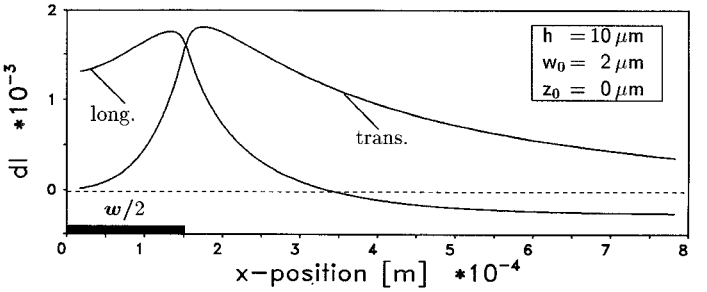

Fig. 10. $\overline{\Delta I}$ of longitudinal and transverse probing with $LiTaO_3$.

The calculated intensity $\overline{\Delta I}$ of longitudinal and transverse probing is depicted in Fig. 10. As shown, a delocation between maximum intensity and location of transmission line edge with increasing value, and less pronounced peak for increasing air gap, is present. However, even at the large probe distances, the proposed simultaneous probing of longitudinal and transverse fields allows the exact determination of the location of the edge within a few μm. It can be shown, that using a 1 μm gap, 30% of the available potential is evaluated, which increases to 65% for a 400 μm thick EO-crystal. Further, the method allows the derivation of correction algorithms.

VIII. Conclusion

The volume-integral method presented can be applied to the case of external and internal electrooptic probing and, yields important results on the introduced transmission characteristic which is described by sensitivity and spatial resolution. In case of external electrooptic sampling, the influence of the probing beam parameters and geometric dimensions of probe tip and its distance to the planar circuit is presented. The described method can be applied to arbitrary inhomogeneous fields and arbitrary optical fields. The method allows the effective optimization of the electrooptic sampling setup for various probing geometries and planar structures, and the implementation of correction algorithms.

References

[1] T. Nagatsuma, T. Shibata, E. Sano, and A. Iwata, "Subpicosecond sampling using a noncontact electro-optic probe," *J. Appl. Phys.*, vol. 66, pp. 4001–4009, Nov. 1989.

[2] M. Y. Frankel, J. F. Whitaker, G. A. Mourou, and J. A. Valdmanis, "Experimental characterization of external electrooptic probes," *IEEE Micro. Guided Wave Lett.*, vol. 1, pp. 60–63, Mar. 1991.

[3] G. N. Ramachandran and S. Ramaseshan, "Crystal Optics," in *Handbuch der Physik, Band 25/I*, S. Flügge (Hrsg). Berlin: Springer-Verlag, 1962, pp. 1–30.

[4] V. Thomas, "Elektrooptische Sonde zur Potentialabtastung in integrierten Hochfrequenzschaltungen," Ph.D. thesis, Technische Universität München, Lehrstuhl für Hochfrequenztechnik, 1991.

[5] M. Rottenkolber, "Theoretischer Beitrag zur Optimierung eines elektrooptischen Abtastkopfes für Mikrowellenschaltungen," M.S. thesis, Technische Universität München, Institut für Hochfrequenztechnik, 1992.

[6] S. Aoshima, H. Takahashi, T. Nakamura, and Y. Tsuchiya, "Noncontact picosecond electro-optic sampling utilizing semiconductor laser pulses," in *33rd SPIE Conf.*, vol. 1155. San Diego, CA., Aug. 6–11, 1989.

[7] T. Nagatsuma and M. Shinagawa, "Picosecond electro-optic probing of high-speed integrated circuits," NTT LSI Laboratories, 1990.

[8] G. D. Monteath, *Applications of Electromagnetic Reciprocity Principle*. Oxford: Pergamon, 1973.
[9] J. L. Freeman, S. R. Jeffries, G. A. Mourou, and J. A. Valdmanis, "Full field modeling of the longitudinal electrooptic probe," *Optics Letters*, vol. 12, pp. 765–766, 1987.
[10] H. A. Haus, *Waves and fields in optoelectronics*. Englewood Cliffs, NJ: Prentice-Hall, 1984.
[11] M. Rottenkolber, W. Thomann, and P. Russer, "Characterization and optimization of electrooptic sampling by volume-integral-method and application of space-harmonic potential," in *MTT-S Symposium*, Atlanta, GA, June 14–16, 1993.

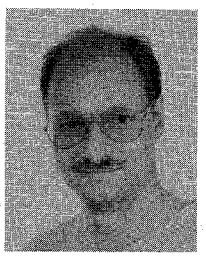

Wolfgang Thomann (M'90) was born in Albstadt, Germany, in 1962. He received the Dipl.-Ing. (FH) degree in 1987 from the Fachhochschule Furtwangen, Germany and the Dipl.-Ing. (Univ.) degree in 1990 from the Technische Universität München, Germany. Since 1990, he has been a Research Assistant at the Technische Universität München. His current research interests are microwave circuits and systems, high-speed electronic and electrooptic sampling, electronic pulse generation, and device modeling.

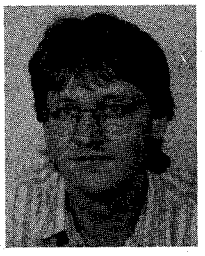

Matthias Rottenkolber was born in München, Germany in 1966. He received the Dipl.-Ing. degree in 1992 from the Technische Universität München, Germany.

Since 1992, he has been with ITEC Consulting, München, Germany. His current research interests are electrooptic systems, holography, and speckle-pattern interferometry.

Peter Russer (SM'81), for a photograph and biography, see this issue, p. 2155.